Structures and Redox Properties of Metal Complexes of the Electron-Deficient Diphosphine Chelate Ligand *R,R*-QuinoxP

Atanu Kumar Das,[†] Ece Bulak,[†] Biprajit Sarkar,[†] Falk Lissner, Thomas Schleid,[†] Mark Niemeyer,[†] Jan Fiedler,[‡] and Wolfgang Kaim*,[†]

Institut für Anorganische Chemie, Universität Stuttgart, Pfaffenwaldring 55, D-70550 Stuttgart, Germany, and J. Heyrovský Institute of Physical Chemistry, v.v.i., Academy of Sciences of the Czech Republic, Dolejškova 3, CZ-18223 Prague, Czech Republic

Received July 25, 2007

The air-stable chiral diphosphine chelate ligand *R,R*-QuinoxP (L; 2,3-bis(*tert*-butylmethylphosphino)-quinoxaline) as developed by Imamoto et al. has been used to obtain the crystallographically characterized complexes (L)$PtCl_2$ (**1**), (L)$PdCl_2$ (**2**), and (L)$Re(CO)_3Cl$ (**3**). Coordination was found to occur via the P donor atoms, as indicated by crystal structures and NMR studies; the quinoxaline N donors do not participate in any coordination to the metals. The stereochemical arrangements observed illustrate the enantioselectivity reported for catalysis involving complexes of L. Electron acceptance by the quinoxaline heterocycle is responsible not only for the improved stability of L toward air but also for rather facile reduction of the complexes to the persistent radical anions $\mathbf{1}^{\bullet-}$ and $\mathbf{3}^{\bullet-}$. In contrast, the reduction to $\mathbf{2}^{\bullet-}$ proceeds irreversibly even at 243 K in the absence of excess chloride. EPR, UV–vis, and IR spectroelectrochemistry was used, when possible, to establish the spin location in the quinoxaline π system with rather small contributions from the metals or the phosphorus nuclei.

Introduction

Chiral 1,4-diphosphine ligands capable of forming five- or six-membered metal chelate rings have long been established as essential components of successful enantioselective catalysis systems, involving especially hydrogenation and C−C bond forming reactions.[1] For practical applications, however, the necessity of working with air-sensitive alkylphosphines has been a drawback, which is why strategies to overcome this inconvenience and simultaneously preserve or even improve the catalytic activity and selectivity have been sought. Imamoto and co-workers have recently presented a class of diphosphine ligands which fulfill these requirements, using the rigid and π-electron-deficient quinoxaline heterocycle as a platform to which the dialkylphosphinosubstituents could be attached in the 2,3-positions.[2,3] The resulting molecules such as 2,3-bis(*tert*-butylmethylphosphino)quinoxaline (QuinoxP)[2] and related diphosphines[3] were employed in connection with rhodium and palladium components for asymmetric hydrogenation and carbon−carbon bond formation.

Considering the tendency of quinoxalines,[4] especially metal-coordinated ones,[5] to undergo reversible electron uptake to form persistent, EPR-detectable radical anion species, we have now used the *R,R* isomer L of QuinoxP in order to structurally establish the transition-metal binding to the P (and not N) donor atoms. The electron transfer behavior of the compounds (L)$PtCl_2$ (**1**), (L)$PdCl_2$ (**2**), and (L)$Re(CO)_3Cl$ (**3**) was investigated by cyclic voltammetry, EPR, UV–vis and IR spectroelectrochemistry. Palladium complexes such as **2** were implicated in the enantioselective catalysis of C-C bond formation.[2]

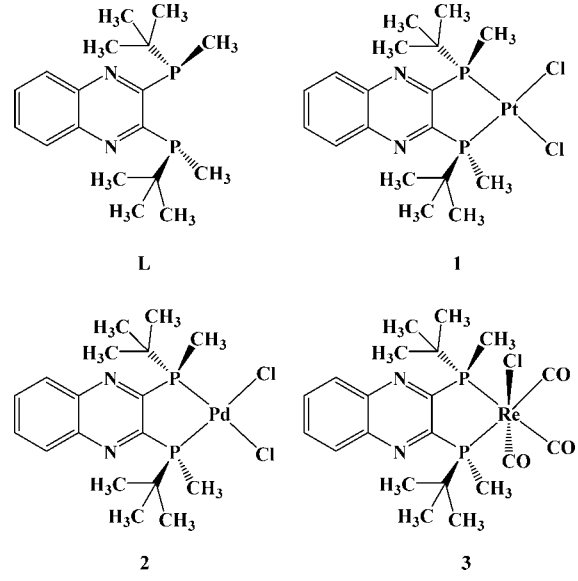

Experimental Section

Instrumentation. EPR spectra at X-band were recorded with a Bruker System EMX instrument. ^1H and ^{31}P NMR spectra were recorded on a Bruker AC 250 spectrometer. IR spectra were obtained using a Nicolet 6700 FT-IR instrument; solid-state IR measurements were performed with an ATR unit (smart orbit with diamond crystal). UV–vis-near-IR absorption spectra were recorded

[†] Universität Stuttgart.
[‡] J. Heyrovský Institute of Physical Chemistry.

(1) (a) Ohkuma, T.; Kitamura, M.; Noyori, R. In *Catalytic Asymmetric Synthesis*, 2nd ed.; Ojima, I., Ed.; Wiley-VCH: New York, 2000; pp 1. (b) Brown, J. M. In *Comprehensive Asymmetric Catalysis*; Jacobsen, E. N., Pfalz, A., Yamamoto, H., Eds.; Springer-Verlag: Berlin, 1999; Vol. 1, pp 121. (c) Crépy, K. V. L.; Imamoto, T. *Top. Curr. Chem.* **2003**, *229*, 1.
(2) Imamoto, T.; Sugita, K.; Yoshida, K. *J. Am. Chem. Soc.* **2005**, *127*, 11934.
(3) Imamoto, T.; Kumada, A.; Yoshida, K. *Chem. Lett.* **2007**, *36*, 500.
(4) Henning, J. C. M. *J. Chem. Phys.* **1966**, *44*, 2139.
(5) (a) Kaim, W. *Chem. Ber.* **1982**, *115*, 910. (b) Kaim, W. *Angew. Chem.* **1983**, *95*, 201; *Angew. Chem., Int. Ed. Engl.* **1983**, *22*, 171. (c) Kaim, W.; Kohlmann, S.; Lees, A. L.; Zulu, M. M. *Z. Anorg. Allg. Chem.* **1989**, *575*, 97.

10.1021/om700755y CCC: $40.75
Publication on Web 01/03/2008

Table 1. Crystallographic Data[a]

	1·CH_2Cl_2	**2**·CH_2Cl_2	**3**
empirical formula	$C_{19}H_{30}Cl_4N_2P_2Pt$	$C_{19}H_{30}Cl_4N_2P_2Pd$	$C_{21}H_{28}ClN_2O_3P_2Re$
molecular mass (g)	685.28	596.59	640.04
cryst syst	monoclinic	monoclinic	monoclinic
temp (K)	100(2)	100(2)	173(2)
space group	$P2_1$	$P2_1$	$C2$
a (Å)	7.9288(2)	7.92520(10)	22.692(4)
b (Å)	15.1703(4)	15.1396(3)	10.5200(2)
c (Å)	10.4448(2)	11.993(2)	10.4390(15)
β (deg)	99.605(2)	99.015(1)	104.375 (12)
V (Å^3)	1247.63(5)	1237.73(4)	2751.9(8)
Z	2	2	4
D_{cal} (g cm^{-3})	1.824	1.601	1.545
μ (mm^{-1})	6.19	1.32	4.650
2θ range (deg)	3.74–56.56	3.30–56.54	2.37–55.00
no. of data collected	19 600	19 367	3403
no. of unique data/R_{int}	6001/0.136	5951/0.105	3314/0.035
no. of data with $I > 2\sigma(I)$ (N_o)	5563	5719	3056
no. of params	262	262	281
$R1$[b]	0.043	0.028	0.028
wR2[c]	0.104	0.081	0.067
GOF[d]	1.051	1.023	0.998
Flack x	−0.006	−0.026	−0.003(10)
max/min residual dens (e/Å^3)	2.31/−1.76	0.80/−0.68	1.06/−1.31

[a] All data were collected using Mo Kα (λ = 0.710 73 Å) radiation. [b] $R1 = \sum(\triangle F_o| - |F_c\triangle)/\sum(|F_o|$. [c] $wR2 = \{\sum[w(F_o - F_c^2)^2]/\sum[w(F_o^2)^2]\}^{1/2}$. [d] $GOF = \{\sum[w(F_o - F_c^2)^2]/(N_o - N_p)\}^{1/2}$.

on J&M TIDAS and Shimadzu UV 3101 PC spectrophotometers. Cyclic voltammetry was carried out in 0.1 M Bu_4NPF_6 solutions using a three-electrode configuration (glassy-carbon working electrode, Pt counter electrode, Ag/AgCl reference) and a PAR 273 potentiostat and function generator. The ferrocene/ferrocenium (Fc/Fc^+) couple served as internal reference. Spectroelectrochemistry was performed using an optically transparent thin-layer electrode (OTTLE) cell.[6] A two-electrode capillary served to generate intermediates for X band EPR studies.[7]

Synthesis. ((*R*,*R*)-(−)-2,3-Bis(*tert*-butylmethylphosphino)quinoxaline)dichloroplatinum (1). To a 63.5 mg amount of the quinoxaline ligand (0.19 mmol) dissolved in 20 mL of dichloromethane was added dropwise a dichloromethane solution of 80 mg (0.19 mmol) of $Pt(dmso)_2Cl_2$. The mixture was stirred at room temperature for 12 h under an argon atmosphere. The solvent was removed under reduced pressure until about 5 mL was left; addition of diethyl ether precipitated the product, which was left at 0 °C overnight to complete precipitation. The solution was then filtered and the solid washed several times with diethyl ether until the filtrate became colorless. The yellow solid was dried to yield 47 mg (82%) of product. Anal. Calcd for $C_{18}H_{28}Cl_2N_2P_2Pt$ (600.37): C, 36.01; H, 4.70; N, 4.67. Found: C, 35.88; H, 4.76; N, 4.41. ^{1}H NMR ($CDCl_3$): δ 1.19 (d, 18H, 6 CH_3, ^3J(P−H) =16.4 Hz), 2.25 (d, 6H, 2 CH_3, ^2J(P−H) = 12.0 Hz, ^3J(Pt−H) = 36.0 Hz), 7.98–8.08 (m, 2H), 8.27–8.37 (m, 2H). ^{31}P NMR ($CDCl_3$): δ 30.65 (s, ^1J(Pt−P) = 3446.5 Hz). UV/vis (CH_2Cl_2; λ_{max}/nm (ϵ/M^{-1} cm^{-1})): 395 sh, 340 (10 590), 329 (9260).

((*R*,*R*)-(−)-2,3-Bis(*tert*-butylmethylphosphino)quinoxaline)dichloropalladium (2). An 22.1 mg amount (0.066 mmol) of $Pd(dmso)_2Cl_2$ in 10 mL of CH_2Cl_2 was added to a 10 mL CH_2Cl_2 solution of 24 mg (0.071 mmol) of quinoxaline, and the mixture was stirred for 2 h. The light yellow solution was concentrated to half its volume. Upon addition of hexane and filtration 15 mg (44.4%) of pale yellow product was obtained after drying. Single crystals were obtained from dichloromethane/hexane as dichloromethane solvate. Anal. Calcd for $C_{19}H_{30}Cl_4N_2P_2Pd$ (596.61): C, 38.25; H, 5.07; N, 4.70%. Found: C, 37.41; H, 5.20; N, 4.35. ^{1}H NMR (CD_2Cl_2): δ 1.24 (d, 18H, 6 CH_3, ^3J(P−H) = 16.6 Hz), 2.23 (d, 6H, 2 CH_3, ^2J(P−H) = 12.0 Hz), 8.04 (m, 2H), 8.32 (m, 2H). ^{31}P NMR (CD_2Cl_2): δ 55.34 (s). UV/vis (CH_2Cl_2; λ_{max}/nm (ϵ/M^{-1} cm^{-1})): 341 (10 340), 329 (8980).

((*R*,*R*)-(−)-2,3-Bis(*tert*-butylmethylphosphino)quinoxaline)tricarbonylchlororhenium (3). A mixture of $Re(CO)_5Cl$ (80 mg, 0.22 mmol) and of the quinoxaline ligand (73.9 mg, 0.22 mmol) in 40 mL of 3:1 toluene−dichloromethane was heated to reflux for 4 h under an argon atmosphere. The solvent was removed under reduced pressure to 10 mL, and a solid was precipitated on addition of diethyl ether at 0 °C. The yellow precipitate was collected and washed several times with diethyl ether and dried to yield 125 mg (88%) of product. Anal. Calcd for $C_{21}H_{28}ClNO_3P_2Re$ (640.06): C, 39.41; H, 4.41; N, 4.38. Found: C, 40.73; H, 4.57; N, 4.17. ^{1}H NMR ($CDCl_3$): δ 1.37 (d, 9H, 3CH_3, ^3J(P−H) = 15.5 Hz), 1.21 (d, 9H, CH_3, ^3J(P−H) = 15.3 Hz), 2.13 (d, CH_3, 3H, ^2J(P−H) = 8.8 Hz), 2.16 (d, CH_3, 3H, ^2J(P−H) = 7.93 Hz), 7.85–7.97 (m, 2H), 8.15–8.27 (m, 2H). ^{31}P NMR ($CDCl_3$): δ 13.01 (d, ^3J(P−P) = 25.5 Hz), 28.10 (d, ^3J(P−P) = 25.5 Hz). UV/vis (CH_2Cl_2; λ_{max}/nm (ϵ/M^{-1} cm^{-1})): 325 (8660), 338 (8960), 390 (sh). IR (CH_2Cl_2; ν(CO)/cm^{-1}): 2032 vs, 1953 s, 1895 s.

Crystallography. Single crystals were obtained as dichloromethane solvates from dichloromethane/hexane (diffusion method) for **1** and **2**, which crystallize in an isostructural way. Data were collected of selected specimens (pale yellow prisms 0.2 × 0.1 × 0.1 mm in both cases) with a NONIUS Kappa CCD diffractometer at 100 K. The structures were solved using direct methods with refinement by full-matrix least squares of F^2, employing the program system SHELXL 97 in connection with absorption correction.[8] All non-hydrogen atoms were refined anisotropically; hydrogen atoms were introduced at appropriate positions. Single crystals of **3** were obtained from dichloromethane−hexane at −25 °C. The X-ray data collection (yellow prisms 0.25 × 0.25 × 0.22 mm) was performed at 173 K on a Siemens P4 four-circle diffractometer with graphite-monochromated Mo Kα radiation (λ = 0.710 73 Å). An empirical absorption correction based on ψ scans of several reflections was applied. Crystallographic data are summarized in Table 1, and selected bond parameters are given in

(6) Krejcik, M.; Danek, M.; Hartl, F. *J. Electroanal. Chem.* **1991**, *317*, 179.

(7) Kaim, W.; Ernst, S. E.; Kasack, V. *J. Am. Chem. Soc.* **1990**, *112*, 173.

(8) (a) Sheldrick, G. M. *Program for Crystal Structure Solution and Refinement*, Universität Göttingen, 1997. (b) Herrendorf, W.; Bärnighausen, H. Program HABITUS, Karlsruhe, Germany, 1993.

Table 2. Selected Bond Lengths (Å) and Bond Angles (deg) of 1 and 2

	M = Pt (**1**)	M = Pd (**2**)
	Bond Lengths	
M−Cl(1)	2.363(2)	2.3654(8)
M−Cl(2)	2.361(2)	2.3639(8)
M−P(2)	2.219(2)	2.2316(8)
M−P(1)	2.219(2)	2.2321(8)
P(1)−C(14)	1.807(9)	1.807(3)
P(1)−C(15)	1.893(8)	1.868(3)
P(2)−C(9)	1.799(8)	1.809(3)
P(2)−C(10)	1.862(7)	1.871(3)
P(1)−C(1)	1.835(9)	1.824(3)
P(2)−C(8)	1.831(8)	1.827(3)
	Bond Angles	
P(1)−M−Cl(1)	91.20(8)	90.56(3)
P(1)−M−Cl(2)	171.11(7)	169.99(3)
P(2)−M−Cl(1)	171.66(7)	169.65(3)
P(2)−M−Cl(2)	91.01(7)	90.07(3)
P(2)−M−P(1)	88.57(8)	87.48(3)
Cl(1)−M−Cl(1)	90.50(7)	93.53(3)
C(9)−P(2)−C(10)	108.9(4)	109.01(16)
C(15)−P(1)−C(14)	108.6(4)	109.01(16)

Table 3. Selected Bond Lengths (Å) and Bond Angles (deg) of 3

Bond Lengths	
Re−Cl	2.503(2)
Re−P(1)	2.483(2)
Re−C(19)	1.939(7)
Re−C(20)	1.937(5)
Re−C(21)	1.968(4)
Re−P(2)	2.462(2)
P(1)−C(14)	1.843(9)
P(1)−C(15)	1.864(8)
P(2)−C(9)	1.820(8)
P(2)−C(10)	1.870(7)
P(1)−C(1)	1.848(2)
P(2)−C(8)	1.847(1)
Bond Angles	
P(1)−Re−Cl	87.71(7)
P(1)−Re−C(20)	171.90(9)
P(1)−Re−C(21)	97.48(1)
P(1)−Re−C(19)	89.31(5)
P(2)−Re−Cl	83.30(7)
P(2)−Re−P(1)	82.50(6)
P(2)−Re−C(20)	89.99(1)
P(2)−Re−C(21)	170.41(5)
P(2)−Re−C(19)	97.78(7)
C(19)−Re−Cl	176.68(6)
C(20)−Re−Cl	94.43(7)
C(21)−Re−Cl	87.11(5)
Re−C(21)−O(21)	176.42(2)
Re−C(20)−O(20)	174.01(4)
Re−C(19)−O(19)	178.37(2)
C(9)−P(2)−C(10)	103.93(8)
C(14)−P(1)−C(15)	103.33(1)

Tables 2 and 3. Further details are provided in the Supporting Information.

Results and Discussion

The free ligand *R,R*-2,3-bis(*tert*-butylmethylphosphino)quinoxaline undergoes an electrochemically reversible one-electron reduction at −2.05 V vs ferrocenium/ferrocene (Table 4); the quinoxaline parent has $E_{1/2} = -2.18$ V. The radical anion produced, $L^{\bullet-}$, shows an only partially resolved EPR signal at $g_{iso} = 2.0030$ with a total spectral width of about 4 mT. Due to the insufficient resolution, the complex spectrum could not yet be analyzed. Nevertheless, this result confirms the π-electron deficiency of quinoxaline,[4] enhanced further by the established electron-withdrawing effect of dialkylphosphino substituents.[9,10]

Treatment of L with standard metal complex precursors yields the three complexes (L)$PtCl_2$ (**1**), (L)$PdCl_2$ (**2**), and (L)$Re(CO)_3Cl$ (**3**); the results of their crystal structure determination are summarized and illustrated in Tables 2 and 3 and Figures 1−3.

The structures show the expected[2] formation of five-membered chelate rings involving two ortho-positioned dialkylphosphino groups (*R* configuration) and the four-coordinate d^8 (**1**, **2**) or six-coordinate d^6 configured metal centers (**3**). The five-membered rings are approximately planar, adopting only a slightly twisted conformation. No intra- or intermolecular metal/quinoxaline interaction was detected. According to the straightforward NMR spectra this arrangement is maintained also in solution; splitting of P-methyl and P-*tert*-butyl ^{1}H NMR signals for **3** reflect the different chemical environments above and below the π plane as a consequence of the *fac*-$Re(CO)_3Cl$ configuration (Figure 3).

The complexes show one-electron electrochemical reduction, facilitated in comparison to that of the free ligand (Table 4). The second reduction could not be observed in CH_2Cl_2 or CH_3CN, suggesting a large comproportionation constant for the intermediate, as would be expected for 1,4-diazine redox systems.[5b] Electron addition proved to be irreversible (EC_{ir} process) even at 243 K for the dichloropalladium complex **2**; addition of excess (0.1 M) Bu_4NCl enhanced the reversibility and allowed us to determine a potential of −1.45 V ($\Delta E = 110$ mV) at a 200 mV/s scan rate. The much more pronounced lability of 4d transition-metal−halide bonds on reduction relative to 5d element analogues is well-known;[11] it can be desirable for some kinds of catalytic activation.[12] The rhenium(I) compound **3** exhibits a partially reversible oxidation (Figure 4) at a potential higher than that for the (irreversible) oxidation of L. This result reflects the involvement of phosphine lone pairs in metal binding and suggests a metal-based oxidation to labile rhenium(II);[13] unfortunately, the spectroelectrochemical mea-

(9) (a) Kaim, W.; Bock, H. *J. Am. Chem. Soc.* **1978**, *100*, 6504. (b) Kaim, W.; Bock, H. *Chem. Ber.* **1981**, *114*, 1576. (c) Gross-Lannert, R.; Kaim, W.; Lechner, U.; Roth, E.; Vogler, C. *Z. Anorg. Allg. Chem.* **1989**, *579*, 47. (d) Giordan, J. C.; Moore, J. H.; Tossell, J. A.; Kaim, W. *J. Am. Chem. Soc.* **1985**, *107*, 5600.

(10) (a) Fenske, D. *Chem. Ber.* **1979**, *112*, 363. (b) Becher, H. J.; Fenske, D.; Heymann, M. *Z. Anorg. Allg. Chem.* **1981**, *475*, 27. (c) Fenske, D.; Becher, H. J. *Chem. Ber.* **1974**, *107*, 117; **1975**, *108*, 2115. (d) Becher, H. J.; Bensmann, W.; Fenske, D. *Chem. Ber.* **1977**, *110*, 315. (e) Fenske, D. *Angew. Chem.* **1976**, *88*, 415; *Angew. Chem., Int. Ed. Engl.* **1976**, *15*, 381. (f) Bensmann, W.; Fenske, D. *Angew. Chem.* **1979**, *91*, 754; *Angew. Chem., Int. Ed. Engl.* **1979**, *18*, 677. (g) Fenske, D.; Christidis, A. *Angew. Chem.* **1981**, *93*, 113; *Angew. Chem., Int. Ed. Engl.* **1981**, *20*, 129. (h) Fenske, D.; Christidis, A. *Z. Naturforsch., B* **1981**, *36*, 518. (i) Fenske, D.; Brandt, K.; Stock, P. *Z. Naturforsch., B* **1981**, *36*, 768. (j) Fenske, D.; Stock, P. *Angew. Chem.* **1982**, *94*, 393; *Angew. Chem., Int. Ed. Engl.* **1982**, *21*, 356; *Angew. Chem. Suppl.* **1982**, 862. (k) Fenske, D.; Bensmann, W. *Z. Naturforsch., B* **1984**, *39*, 1819. (l) Fenske, D.; Bensmann, W. *Z. Naturforsch., B* **1985**, *40*, 1093. (m) Duffy, N. W.; Nelson, R. R.; Richmond, M. G.; Rieger, A. L.; Rieger, P. H.; Robinson, B. H.; Tyler, D. R.; Wang, J. C.; Yang, K. *Inorg. Chem.* **1998**, *37*, 4849. (n) Braden, D. A.; Tyler, D. R. *Organometallics* **2000**, *19*, 3762.

(11) Frantz, S.; Reinhardt, R.; Greulich, S.; Wanner, M.; Fiedler, J.; Duboc-Toia, C.; Kaim, W. *Dalton Trans.* **2003**, 3370.

(12) (a) Kölle, U.; Grätzel, M. *Angew. Chem.* **1987**, *99*, 572; *Angew. Chem., Int. Ed. Engl.* **1987**, *26*, 568. (b) Kölle, U.; Kang, B.-S.; Infelta, P.; Compte, P.; Grätzel, M. *Chem. Ber.* **1989**, *122*, 1869. (c) Chardon-Noblat, S.; Cosnier, S.; Deronzier, A.; Vlachopoulos, N. *J. Electroanal. Chem.* **1993**, *352*, 213. (d) Westerhausen, D.; Herrmann, S.; Hummel, W.; Steckhan, E. *Angew. Chem.* **1992**, *104*, 1496; *Angew. Chem., Int. Ed. Engl.* **1992**, *321*, 1529. (e) Kaim, W.; Reinhardt, R.; Sieger, M. *Inorg. Chem.* **1994**, *33*, 4453.

(13) (a) Klein, A.; Vogler, C.; Kaim, W. *Organometallics* **1996**, *15*, 236. (b) Hartmann, H.; Scheiring, T.; Fiedler, J.; Kaim, W. *J. Organomet. Chem.* **2000**, *604*, 267. (c) Frantz, S.; Fiedler, J.; Hartenbach, I.; Schleid, Th.; Kaim, W. *J. Organomet. Chem.* **2004**, *689*, 3031. (d) Knödler, A.; Wanner, M.; Fiedler, J.; Kaim, W. *Dalton Trans.* **2002**, 3079.

Table 4. Electrochemical and Spectroscopic Properties of the Ligand L and Its Complexes

	L^n	$\mathbf{1}^n$	$\mathbf{2}^n$	$\mathbf{3}^n$
E(red)[a]	−2.05 ($E_{1/2}$)	−1.56 ($E_{1/2}$)	−1.78 ($E_{p,c}$)[b]	−1.70 ($E_{1/2}$)
E(ox)[a]	+0.36 ($E_{p,a}$)	>1.5	>1.5	+1.11 ($E_{1/2}$)
ν(CO)[c] ($n = 0$)				2032 vs, 1953 s, 1895 s
ν(CO)[c] ($n = -1$)				2014 vs, 1928 s, 1877 s
λ_{max}/ϵ[d] ($n = 0$)	n.a.	340/10.59, 329/9.27, 395 (sh),329/9.26	341/10.34, 329/8.98	338/8.96, 325/8.66, 390 (sh)
λ_{max}/ϵ[d] ($n = -1$)	n.a.	n.a.	n.a.	269/11.40, 289/10.86, 335/8.00,360 (sh), 563/4.39
g ($n = -1$)	2.0030[e]	2.0045[f]	n.a.	2.0032,[f] 2.0034[g]
A ($n = -1$)[h]	partially resolved (40 G spectral width)	$A(^{195}Pt) = 24$ (1Pt),[f] $A(^{14}N) = 5.8$ (2N), $A(^{1}H) = 1.7$ (2H),[g] $A(^{31}P) = 1.7$ (2P)[j]	n.a.	partially resolved (70 G spectral width)

[a] In CH_2Cl_2/0.1 M Bu_4NPF_6. Potentials are given in V vs $(C_5H_5)_2Fe^{+/0}$, with half-wave ($E_{1/2}$) or peak potentials ($E_{p,c}$, $E_{p,a}$) for irreversible processes. [b] At −30 °C; $E_{1/2} = -1.45$ V in the presence of 0.1 M Bu_4NCl. [c] Carbonyl stretching bands in cm^{-1}. [d] Absorption maxima (λ_{max}) in nm/molar extinction coefficients (ϵ) in 10^3 M^{-1} cm^{-1}. [e] In CH_3CN/0.1 M Bu_4NPF_6 at 298 K. [f] In CH_2Cl_2/0.1 M Bu_4NPF_6 at 298 K. No g factor splitting observed at 110 K. [g] In CH_2Cl_2/0.1 M Bu_4NPF_6 at 110 K. No g factor splitting observed at 110 K. [h] EPR coupling constants in G (1 G = 10^{-4} T). [j] Tentative assignment (cf. text).

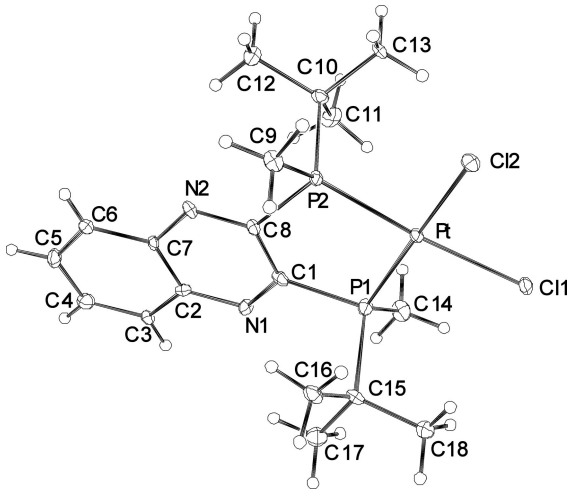

Figure 1. Molecular structure of **1** in the crystal of $\mathbf{1}\cdot 2CH_2Cl_2$ (thermal ellipsoids including 30% probability).

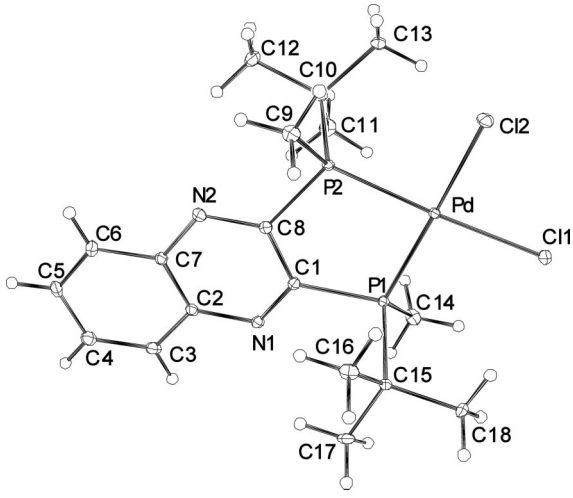

Figure 2. Molecular structure of **2** in the crystal of $\mathbf{2}\cdot 2CH_2Cl_2$ (thermal ellipsoids including 30% probability).

surements suffered from extensive decomposition of electrogenerated $\mathbf{3}^+$.

Reversible one-electron reduction could be monitored by EPR, IR, and UV–vis spectroelectrochemistry for the Re^I species **3** and by EPR for the platinum(II) complex **1**. While all compounds display metal-to-(acceptor) ligand charge transfer (MLCT) absorptions in the near-UV region (Table 4), the formation of $\mathbf{3}^{\bullet-}$ is accompanied by the emergence of an intense

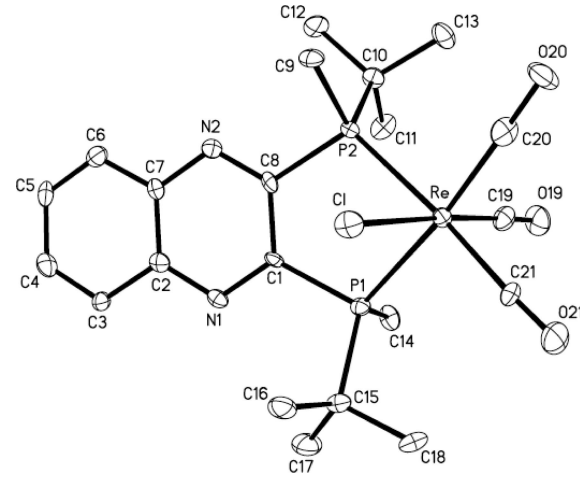

Figure 3. Molecular structure of **3** in the crystal (thermal ellipsoids including 30% probability).

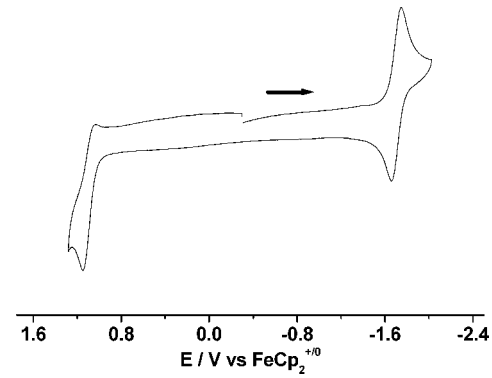

Figure 4. Cyclic voltammetry of **3** in dichloromethane/0.1 M Bu_4NPF_6 at a 100 mV/s scan rate.

band system in the visible region (Figure 5). Quinoxaline radical anions are distinguished by long-wavelength absorptions around 600 nm;[14] we therefore assign the observed bands in $\mathbf{3}^{\bullet-}$ to intraligand and (bathochromically shifted) MLCT transitions. The rather marginal involvement of the *fac*-$Re(CO)_3Cl$ fragment in the spin distribution on reduction of **3** is also evident from the comparatively small low-energy shift of about 20 cm^{-1} for the three CO stretching bands (Figure 6, Table 4). For comparison, (abpy)$Re(CO)_3Cl$ (abpy = 2,2′-azobis(pyridine)) shows an average shift of 40 cm^{-1} on reduction.[13b,c]

(14) Shida, T. *Electronic Absorption Spectra of Radical Ions*; Elsevier: Amsterdam, 1988; p 176.

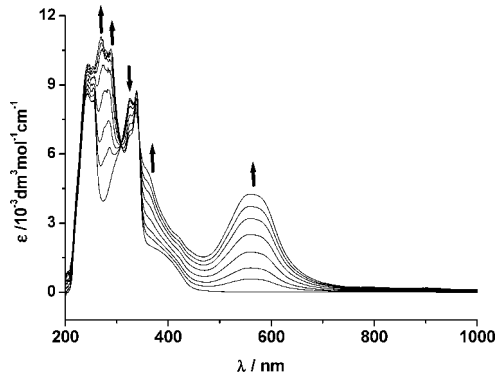

Figure 5. UV–vis spectroelectrochemistry of the conversion of **3** to $\mathbf{3}^{\bullet-}$ in dichloromethane/0.1 M Bu_4NPF_6.

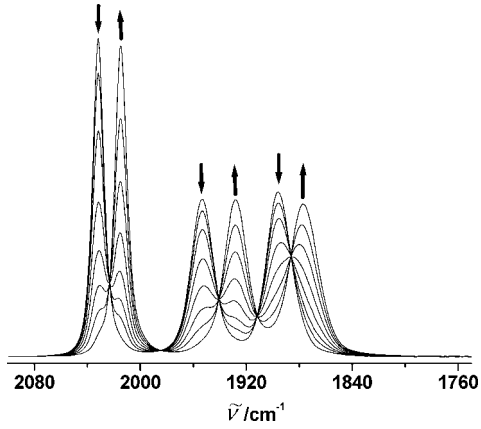

Figure 6. IR spectroelectrochemistry of the conversion of **3** to $\mathbf{3}^{\bullet-}$ in dichloromethane/0.1 M Bu_4NPF_6.

EPR studies of radical complexes with heavy transition metals such as Pt[15–18] or Re[13,19] can provide sizable effects, including *g* factor shifts, *g* factor anisotropy, and metal hyperfine coupling. While the former is caused by the large spin–orbit coupling constants of these ions,[20] both the ^{195}Pt (33.8% natural abundance, $I = {}^1/_2$) and ^{185,187}Re isotopes (100%, $I = {}^5/_2$, very similar nuclear magnetic moments) are distinguished by unusually large isotropic hyperfine coupling constants.[20] The EPR spectra of $\mathbf{1}^{\bullet-}$ and $\mathbf{3}^{\bullet-}$ (Figure 7, Table 4) show *g* values close

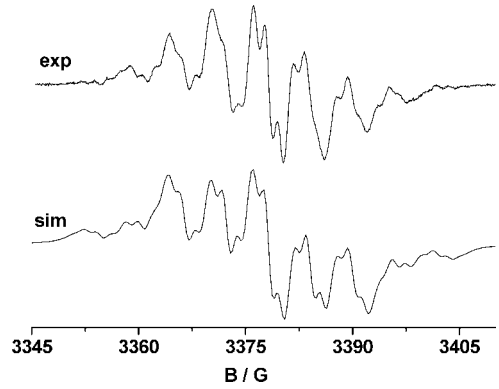

Figure 7. EPR spectrum of electrochemically generated $\mathbf{1}^{\bullet-}$ at room temperature in dichloromethane/0.1 M Bu_4NPF_6 (top, X band at 9.4776 GHz) with simulation (bottom, 0.1 G line width, parameters from Table 4).

to that of the ligand radical anion ($g = 2.0030$), confirming the marginal contribution of the metals to the singly occupied molecular orbital. This result is supported by the lack of detectable *g* anisotropy at X band frequency (9.5 GHz). Whereas $\mathbf{3}^{\bullet-}$ did not show sufficient EPR resolution for hyperfine structure analysis, except for significantly higher spectral width due to ^{185,187}Re splitting at the order of about 5 G, the complex ion $\mathbf{1}^{\bullet-}$ exhibits the typically large ^{14}N ($I = 1$) coupling parameter of quinoxalines (5.7 G)[4,5] as well as smaller ^{1}H and possibly ^{31}P splitting. Both kinds of nuclei have $I = {}^1/_2$; quinoxaline anion was reported with 3.3 G (2H), 2.4 G (2H), and 1.45 G (2H).[5] Considering the relatively large π spin population in the 2,3-positions of quinoxaline anions,[5] we made the tentative assginment given in Table 4. The radical $\mathbf{1}^{\bullet-}$ exhibits a sizable ^{195}Pt hyperfine coupling of 24 G (Figure 7, Table 4). Although semidione complexes of imidazolyl-coordinated $PtCl_2$ have even smaller $a(^{195}\text{Pt})$ hyperfine splitting,[17] the value of 24 G is still below the approximately 40–50 G of typical $(\text{Het}^{\bullet-})PtCl_2$ complexes, e.g. the heterocycles Het = bpy, bpym,[15,16] and is certainly much smaller than what would be expected for mononuclear platinum(I) species.[21]

All of these results thus support a formulation of $(L^{\bullet-})MX_n$ in which the electron has been added to the heterocyclic π system of the molecule (spin localization on quinoxaline[5]), whereas the metal coordination takes place at the stereochemically modified phosphino substituents, where relatively little spin density is present. Such a situation, the separation of coordination site and primary electron transfer site, is partially reminiscent of that in complexes of bis(diphosphino)maleic anhydrides[10] and dipyrido[3,2-*a*:2′,3′-*c*]phenazine (dppz)[18a,22] and related ligands, where the added electron is also *not* localized at the coordination site. In fact, the structures of L and dppz exhibit obvious similarities, although the larger π system of dppz and the lower acceptor level of the phenanthroline section as compared to phosphinyl substituents make a difference.

The decoupling of the electron transfer site from the coordination site in potentially catalytic metal species may become of interest when working under strongly reducing conditions such as hydride-involving reactions.

(15) (a) MacGregor, S. A.; McInnes, E.; Sorbie, R. J.; Yellowlees, L. J. In *Molecular Electrochemistry of Inorganic, Bioinorganic and Organometallic Compounds*; Pombeiro, A. J. L., McCleverty, J. A., Eds.; Kluwer Academic: Dordrecht, The Netherlands, 1993; p 503. (b) Collison, D.; McInnes, E. J. L.; Mabbs, F. E.; Taylor, K. J.; Welch, A. J.; Yellowlees, L. J. *J. Chem. Soc., Dalton Trans.* **1996**, 329. (c) McInnes, E. J. L.; Farley, R. D.; Macgregor, S. A.; Taylor, K. J.; Yellowlees, L. J.; Rowlands, C. C *J. Chem. Soc., Faraday Trans.* **1998**, *94*, 2985. (d) McInnes, E. J. L.; Farley, R. D.; Rowlands, C. C.; Welch, A. J.; Rovatti, L.; Yellowlees, L. J. *J. Chem. Soc., Dalton Trans.* **1999**, 4203.

(16) Kaim, W.; Dogan, A.; Wanner, M.; Klein, A.; Tiritiris, I.; Schleid, Th.; Stufkens, D. J.; Snoeck, T. L.; McInnes, E. J. L.; Fiedler, J.; Zalis, S. *Inorg. Chem.* **2002**, *41*, 4139.

(17) Bulak, E.; Leboschka, M.; Schwederski, B.; Sarper, O.; Varnali, T.; Fiedler, J.; Lisssner, F.; Schleid, W.; Kaim, W *Inorg. Chem.* **2007**, *46*, 5562.

(18) (a) Kaim, W.; Klein, A. *Organometallics* **1995**, *14*, 1176. (b) Hasenzahl, S.; Hausen, H.-D.; Kaim, W. *Chem. Eur. J.* **1995**, *1*, 95. (c) Vogler, C.; Schwederski, B.; Klein, A.; Kaim, W. *J. Organomet. Chem.* **1992**, *436*, 367.

(19) (a) Kaim, W.; Kohlmann, S. *Chem. Phys. Lett.* **1987**, *139*, 365. (b) Frantz, S.; Hartmann, H.; Doslik, N.; Wanner, M.; Kaim, W.; Kümmerer, H.-J.; Denninger, G.; Barra, A.-L.; Duboc-Toia, C.; Fiedler, J.; Ciofini, I.; Urban, C.; Kaupp, M. *J. Am. Chem. Soc.* **2002**, *124*, 10563.

(20) Weil, J. A.; Bolton, J. R. *Electron Paramagnetic Resonance*, 2nd ed.; Wiley-Interscience: Hoboken, NJ, 2007.

(21) Braterman, P. S.; Song, J.-L.; Wimmer, F. M.; Wimmer, S.; Kaim, W.; Klein, A.; Peacock, R. D. *Inorg. Chem.* **1992**, *31*, 5084.

(22) (a) Fees, J.; Kaim, W.; Moscherosch, M.; Matheis, W.; Klima, J.; Krejcik, M.; Zalis, S. *Inorg. Chem.* **1993**, *32*, 166. (b) Klein, A.; Scheiring, T.; Kaim, W. *Z. Anorg. Allg. Chem.* **1999**, *625*, 1177. (c) Fees, J.; Ketterle, M.; Klein, A.; Fiedler, J.; Kaim, W. *J. Chem. Soc., Dalton Trans.* **1999**, 2595.

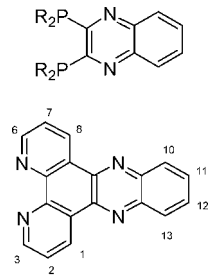

dppz

Conclusion

While the coordination of *R,R*-quinoxP with complex fragments containing d^6 and d^8 configured transition metals via the chelating P donor atoms is not unexpected, the facile reduction to stable radical anion complexes, at least for the 5d element species involving Re(I) and Pt(II), is remarkable. EPR and other spectroelectrochemical methods indicate the primary localization of the unpaired electron in the quinoxaline heterocycle with rather little spin delocalization to the metal centers via the phosphorus atoms. In this respect the complexes resemble other phosphino-substituted organic radical ligands[10] or molecules such as dipyrido[3,2-*a*:2′,3′-*c*]phenazine (dppz),[18a,22] where the coordinating (chelating) group and the spin-bearing section are spatially separated and electronically decoupled, a behavior which may be exploited under strongly reducing situations. Having established the basic structural and electronic features of a QuinoxP ligand in three coordination compounds, we shall direct our future efforts to more catalytically relevant species, involving other transition metals and including less stable intermediates.

Acknowledgment. This work was supported by grants from Deutsche Forschungsgemeinschaft, by the Fonds der Chemischen Industrie, by the European Union (COST D35), and by the Land Baden-Württemberg. We also thank Johnson Matthey for a generous loan of chemicals.

Supporting Information Available: CIF files giving X-ray crystallographic data for **1**−**3**. This material is available free of charge via the Internet at http://pubs.acs.org.

OM700755Y